A Muscle Model Incorporating Fiber Architecture Features for the Estimation of Joint Stiffness During Dynamic Movement

Cop, Christopher P.; Schouten, Alfred C.; Koopman, Bart F.J.M.; Sartori, M.

DOI
10.1007/978-3-030-70316-5_81

Publication date
2022

Document Version
Final published version

Published in
Converging Clinical and Engineering Research on Neurorehabilitation IV

Citation (APA)
Cop, C. P., Schouten, A. C., Koopman, B. F. J. M., & Sartori, M. (2022). A Muscle Model Incorporating Fiber Architecture Features for the Estimation of Joint Stiffness During Dynamic Movement. In D. Torricelli, M. Akay, & J. L. Pons (Eds.), *Converging Clinical and Engineering Research on Neurorehabilitation IV: Proceedings of the 5th International Conference on Neurorehabilitation (ICNR2020), October 13–16, 2020* (pp. 507-511). (Biosystems and Biorobotics; Vol. 28). Springer. https://doi.org/10.1007/978-3-030-70316-5_81

A Muscle Model Incorporating Fiber Architecture Features for the Estimation of Joint Stiffness During Dynamic Movement

Christopher P. Cop, Alfred C. Schouten, Bart F. J. M. Koopman, and M. Sartori

Abstract Quantifying human joint stiffness *in vivo* during movement remains challenging. Well established stiffness estimation methods include system identification and the notion of quasi-stiffness, with experimental and conceptual limitations, respectively. Joint stiffness computation via biomechanical models is an emerging solution to overcome such limitations. However, these models make assumptions that hamper their generalization across muscle architectures. Here we present a stiffness formulation that considers the muscle's pennation angle, and its comparison to a simpler formulation that does not. Model-based stiffness estimates are evaluated against joint-perturbation-based system identification. Results on muscles with different pennation angle show that our formulation seamlessly adjusts the muscle-tendon units' stiffness depending on their architecture. At the joint level, our new model improved the stiffness estimations. Our study's relevance is the creation and validation of a modeling formulation that does not require joint perturbation. This will enable better estimations and understanding of stiffness properties and human movement.

1 Introduction

JOINT stiffness is a biomechanical property that dictates how human limbs interact with the environment. The mechanisms the neuromuscular system uses to modulate it and to provide stability in response to perturbations are not understood yet. Hence, over the last decades there has been a growing interest to quantify human *in vivo* joint stiffness.

This work has been funded by ERC Starting Grant INTERACT (803035).

C. P. Cop (✉) · A. C. Schouten · B. F. J. M. Koopman · M. Sartori
Department of Biomechanical Engineering, University of Twente, Twente, The Netherlands
e-mail: c.p.cop@utwente.nl

A. C. Schouten
Department of Biomechanical Engineering, Delft University of Technology, Delft, The Netherlands

D. Torricelli et al. (eds.), *Converging Clinical and Engineering Research on Neurorehabilitation IV*, Biosystems & Biorobotics 28,
https://doi.org/10.1007/978-3-030-70316-5_81

Joint stiffness has been mostly studied via system identification (Sys. Id.) techniques or using a surrogate concept, i.e. quasi-stiffness. Despite their numerous advantages, both methodologies entail major limitations. On the one hand, Sys. Id. requires an experimental setup in which the joint is externally perturbed. This makes it an undesirable method to study natural movements. On the other hand, quasi-stiffness does not solely represent the position-dependent component of joint impedance, i.e. joint stiffness, as quasi-stiffness also includes velocity- and activation-dependent components.

To overcome these limitations, we propose a stiffness formulation based on biomechanical modeling to estimate joint stiffness in static and dynamic tasks [1]. The idea is to compute joint stiffness by estimating and projecting the stiffness of its constituting elements. However, assumptions and simplifications are often required to model such elements, e.g. the muscle's pennation angle is not considered in the stiffness computation.

In this work we present a joint stiffness model formulation that considers the pennation angle of the modeled muscle-tendon units (MTUs). Moreover, we show the effect of including the pennation angle in the computation of MTU stiffness in muscles with different pennation angle. Lastly. we compare the performance of our new formulation to a simpler model that does not take the pennation angle into account in the stiffness computation. Remarkably, model-based stiffness estimates are directly compared to perturbation-based time-varying system identification values derived from the same subjects and motor tasks. This provides a thorough validation means for our proposed methodology.

2 Methods

2.1 Data Collection

Data from five healthy young subjects (age: 24.2 ± 1.0 years; height: 1.78 ± 0.06 m; weight: 70.0 ± 5.4 kg) were used in this study. Ethical approval was granted by the Ethics Committee of the University of Twente and the participants gave written informed consent.

The subjects' right foot was attached to an admittance controlled dynamometer. The ankle's angle and torque were measured in dynamic movement trials in which the subject tracked a sinusoidal plantar-dorsi flexion angle target (amplitude: 0.15 rad, frequency: 0.6 Hz). Position perturbations, with an amplitude of 0.03 rad and a switching time of 0.15 s, were applied to the ankle in a pseudo-random manner. Electromyography (EMG) signals from five lower leg muscles were acquired: soleus, gastrocnemius lateralis/medialis, peroneus, and tibialis anterior. More details in [2].

2.2 Joint Stiffness Models

The EMG-driven musculoskeletal model shown in [1] was adapted to compute the subject's right ankle stiffness. First, a generic model was calibrated to obtain subject-specific MTU parameters. Then, the ankle joint stiffness (K^J) was computed from the stiffness of its constituting MTUs:

$$K^J = \sum_{\mathrm{i}=1}^{\#mtu} (K_i^{mtu} \cdot r_i^2 - \frac{\partial r_\mathrm{i}}{\partial \theta^A} \cdot F_i) \tag{1}$$

where F_i, r_i and K_i^{mtu} represent the force, moment arm and stiffness, respectively, of the ith MTU spanning the plantar-dorsi flexion degree of freedom of the ankle, and θ^A is the ankle angle in the saggital plane.

MTU stiffness, K^{mtu}, equals the tendon stiffness, K^t, in series with the equivalent muscle fiber stiffness along the tendon's line of action, K_eq^m, i.e. $K^{mtu} = \left(K^{t^{-1}} + K_\mathrm{eq}^{m^{-1}}\right)^{-1}$

Based on the work presented in [3], the equivalent stiffness of a muscle along the tendon's line of action is:

$$K_{eq}^m = \frac{dF_{eq}^m}{dl_{eq}^m} = \frac{d}{dl_{eq}^m}(F^\mathrm{m}\cos\alpha) = \frac{d}{dl_{eq}^m}\left(F^\mathrm{m}\frac{l_{eq}^m}{l^m}\right) = \cdots$$
$$\cdots = \frac{dF^m}{dl^m}\cos^2\alpha + \frac{F^m}{l^m}\sin^2\alpha \tag{2}$$

where F_{eq}^m and l_{eq}^m are the force and length, respectively, of the muscle fiber along the direction of the tendon's line of action, F^m and l^m are the force and length, respectively, of the muscle fiber along its axis, and α represents the muscle fiber's pennation angle. All aforementioned parameters are estimated by the EMG-driven musculoskeletal model.

Two different models were used in this study: the model described in (1) and (2) that takes the pennation angle into account, i.e. model A, and a simpler model, as presented in [1], that does not account for pennation angle in the stiffness computation and thus considers $K_\mathrm{eq}^m = \frac{dF^m}{dl^m}$, i.e. model B.

2.3 Data Analysis

Reference joint stiffness values were obtained using a closed-loop ensemble-based time-varying Sys. Id. method extensively described in [4].

At the MTU level, we quantified the difference in magnitude between models A and B by computing their root mean squared error normalized by the maximum stiffness value (nRMSE) for two MTUs with different pennation angle at optimal fiber length: the tibialis anterior ($\alpha \approx 5°$), and the soleus ($\alpha \approx 25°$).

At the joint level, the results obtained with models A and B were compared to the reference, both in magnitude and in shape, using the root mean squared error (RMSE) and the coefficient of determination (R^2), respectively.

3 Results

We show stiffness estimations at the MTU level for a single subject (Fig. 1a), and at the joint level for the average across all five subjects (Fig. 1b).

At the MTU level, the nRMSEs for the soleus and the tibialis anterior were 0.03 and 0.004, respectively (Fig. 1a).

At the joint level, the stiffness estimations of models A and B were compared to the reference (Fig. 1b). For the average across all five subjects, the R^2 and RMSE values were 0.56 and 3.48 N·m/rad, repectively, for model A, and 0.47 and 4.68 N·m/rad, repectively, for model B.

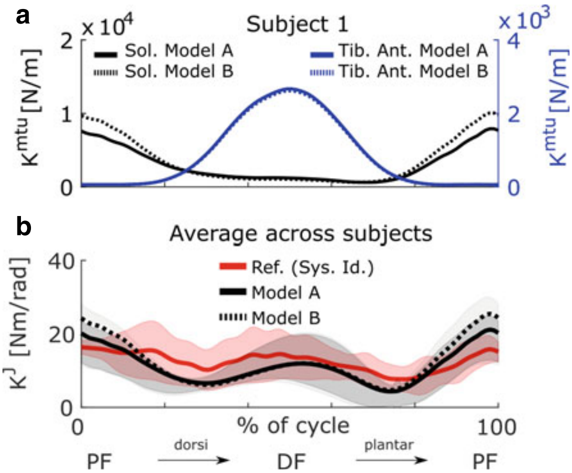

Fig. 1 **a** MTU stiffness of the soleus (black) and the tibialis anterior (blue) muscles computed by models A (solid lines) and B (dotted lines). Note that this plot has two axes of ordinates: one corresponding to the soleus (left) and one corresponding to the tibialis anterior (right). **b** Joint stiffness estimates averaged across all five subjects of model A (solid line), model B (dotted line), and the reference stiffness estimate obtained via system identification (red). The shaded area corresponds to the standard deviation

4 Discussion

To the best of our knowledge this work shows, for the first time, a joint stiffness model that considers pennation angle (i.e. model A) and is directly validated against Sys. Id..

We demonstrate that our proposed joint stiffness formulation can capture multiple muscle architectures simultaneously (Fig. 1a), and seamlessly adjust the equivalent muscle fiber stiffness according to time-varying changing pennation angle (2).

Figure 1b shows how model A improved joint stiffness estimation compared to model B. Interestingly, in the proximity of the dorsiflexion peak of the task (around 50% of the cycle), models A and B compute a similar joint stiffness profile, because most of the dorsiflexion stiffness comes from the tibialis anterior, i.e. a muscle with small α (2).

The largest discrepancy of models A and B is found around the task's plantarflexion peak (around 0 and 100% of the cycle), because the calf muscles, which are usually pennated, contribute to the joint's plantarflexion stiffness (2).

Our results indicate that including the pennation angle in the joint stiffness computation enables better estimations within the plantar-dorsi flexion cycle. This may have implications for the estimation of stiffness during more advanced motor tasks involving complex interplay between pennated and fusiform muscles, e.g. locomotion, stair climbing, etc.

5 Conclusion

Here we presented the first results of an EMG-driven joint stiffness model that takes pennation angle into account and is directly validated. Despite their preliminary nature, our results seem to indicate that including more information on muscle architecture has an impact on joint stiffness estimation and generalization. This will bring us one step further in the understanding of movement neuromechanics.

References

1. M. Sartori, M. Maculan, C. Pizzolato, M. Reggiani, D. Farina, Modeling and simulating the neuromuscular mechanisms regulating ankle and knee joint stiffness during human locomotion. J. Neurophys. **114**(4), 2509–2527 (2015)
2. C.P. Cop, Model-based estimation of ankle joint stiffness during dynamic tasks: a validation-based approach, in *41st Annual International Conference of the IEEE Engineering in Medicine and Biology Society (EMBC)*, vol. 2019, Berlin, Germany (2019), pp. 4104–4107
3. T. Jenkins, M. Bryant, Pennate actuators: force, contraction and stiffness. Bioinspiration Biomim. **15**(4), 046005 (2020)
4. Moya-Esteban A, Estimation of time-varying ankle joint stiffness under dynamic conditions via system identification techniques, in *41st Annual International Conference of the IEEE Engineering in Medicine and Biology Society (EMBC)*, vol. 2019, Berlin, Germany (2019), pp. 2119–2122